Ecological Indicators 133 (2021) 108426

Contents lists available at ScienceDirect

Ecological Indicators

journal homepage: www.elsevier.com/locate/ecolind

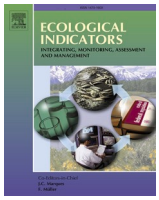

Original Articles

Using remote sensing to forecast forage quality for cattle in the dry savannas of northeast Australia

M.J. Pringle [a,*], P.J. O'Reagain [b], G.S. Stone [a], J.O. Carter [a], T.G. Orton [a,c], J.J. Bushell [b]

[a] Department of Environment and Science, GPO Box 2454, Brisbane, QLD 4001, Australia
[b] Department of Agriculture and Fisheries, PO Box 976, Charters Towers, QLD 4820, Australia
[c] The University of Queensland, School of Agriculture and Food Sciences, St Lucia, QLD 4072, Australia

ARTICLE INFO

Keywords:
faecal NIR spectroscopy
Pasture digestibility
Rangelands

ABSTRACT

In the dry savannas of northeast Australia, forage quality is just as important for cattle production as forage quantity. The seasonal trend of forage quality is broadly predictable by land managers, but it is more difficult to predict the point when quality—which depends on local climate, management, and pasture condition—falls below the requirement for animal maintenance. In this study we use statistical modelling to forecast how forage quality might change at the crucial time of year, i.e., as the summer wet season transitions to the dry winter. We do this with the aid of historical information associated with a long-term cattle-grazing trial in the dry savannas. We combined multiple years of two measures of forage quality (dietary crude protein and *in vivo* dry-matter digestibility; respectively DCP and DMD) and ground cover information (specifically the ratio of 'green grass' cover to 'dead (i.e., non-photosynthetic) grass' cover, derived from an archive of Landsat satellite imagery) into a linear mixed model that explicitly considered the correlations with time and between variables. DCP and DMD were estimated by near-infrared spectroscopy of fresh faecal samples; values did not have to be temporally coincident with the satellite imagery. With the end of May considered a nominal decision-point, we forecast monthly averages of forage quality for June to August, over a 12-year period at the study site. Over all months and all years, the median absolute error of the forecasts was DCP = 0.86%, and DMD = 0.95%. The remote sensing information served as a correlated, oft-sampled covariate that helped to guide the forecasts of forage quality. We propose summarising the forecasts (and their uncertainty) as a near-real-time graphical tool for decision-support. Such a product could potentially benefit cattle-grazing enterprises in the northeast of Australia, enabling more timely management of herds through the dry season.

1. Introduction

Forage quality, as distinct from quantity, is a major constraint to cattle production in the dry savannas of northern Australia. Forage quality is highest during the summer wet season, but declines rapidly when pastures senesce at the onset of the long dry season (McCown, 1981). Cattle can consequently lose body condition and substantial mass during the dry season, even if there appears to be abundant forage (Norman, 1965; Siebert and Kennedy, 1972). The seasonal variability of forage quality is superimposed on a background of highly variable rainfall, with northern Australia marked by runs of multi-year wet or dry periods (McKeon et al., 2021).

It has long been known that forage quality in northern Australia is directly related to the availability of green leaf (McCown, 1981; McIvor, 1981; Poppi et al., 1981). The seasonal trend of forage quality is thus broadly predictable, but the nature of the transition to low-quality forage can vary markedly, depending on the distribution and amount of rainfall (McCown, 1981). For example, very wet years with large growth events can lead to nutrient dilution, while the converse may be true in droughts.

Managers can respond to the decline in forage quality by marketing cattle early, moving the cattle, or providing supplements. In the dry savannas, non-protein nitrogen, in the form of urea (Callaghan et al., 2014), is widely used as a supplement when dietary crude protein (DCP) is perceived as limiting. When energy in the diet is perceived as limiting, supplements such as molasses, often mixed with urea, may also be considered for animals with higher energy requirements (Callaghan et al., 2014). Deploying supplements before they are actually required is

* Corresponding author.
E-mail address: matthew.pringle@qld.gov.au (M.J. Pringle).

https://doi.org/10.1016/j.ecolind.2021.108426
Received 1 April 2021; Received in revised form 23 November 2021; Accepted 26 November 2021
Available online 30 November 2021

an unnecessary cost. Conversely, delaying supplementation too long can result in reduced production.

A key challenge facing land managers in the dry savannas is thus to assess forage quality in an accurate and timely matter. Typically, this is done vaguely, using a combination of cues such as pasture greenness, rainfall received (and forecast), soil moisture, and animal condition. The last may seem an obvious proxy, but can be associated with large uncertainty (Fordyce et al., 2013; Tolleson et al., 2020). The challenge is exacerbated by extremely large grazing properties (typically 20,000–500,000 ha) and widely dispersed herds. The spatial heterogeneity of large paddocks, coupled with the spatial variability of rainfall, adds further complexity. With access to paddocks usually limited, roadside visual assessments of forage quality are unlikely to be representative of a paddock as a whole. While some land managers may monitor forage quality via faecal near-infrared spectroscopic analysis (fNIRS; Dixon and Coates, 2009), samples still need to be collected and dispatched for analysis, which involves time and cost.

An obvious potential solution is to use satellite-derived information, such as the Normalised Difference Vegetation Index (NDVI; Tucker, 1979) or the Enhanced Vegetation Index (EVI; Huete et al., 2002) as a proxy for forage quality (Pettorelli et al., 2011). Both NDVI and EVI have been used to study the foraging behaviour of wild ungulates, including buffalo in the savannas of Africa (Ryan et al., 2012) and Australia (Campbell et al., 2021), chamois in Europe (Villamuelas et al., 2016) and bighorn sheep and bison in the USA (Creech et al., 2016; Geremia et al., 2019). There are fewer published applications that focus on domestic ungulates like cattle and sheep. Notable studies in this space are Phillips et al. (2009), Zengeya et al. (2013), and Panda et al. (2020), who each calibrated a variable related to forage quality—respectively, a C:N ratio, N concentration, and extractable condensed tannin—with a remote sensing-derived vegetation index, and extrapolated the results across their study areas. While insightful, these three studies were each limited to, at most, a single growing season, hence the inter-annual variability of forage quality was not considered. In Queensland's rangelands, Barnetson et al. (2020) found that forage quality for grazing animals was correlated with the red and red-edge regions of the electromagnetic spectrum.

The vast archive of freely available Landsat imagery (landsat.gsfc.nasa.gov) provides a means to investigate—in greater depth than has yet been attempted—the relations with forage quality. In this study we combine Landsat imagery with 23 years of forage quality data from a long-term grazing trial. In contrast to some previous studies, we determine forage quality by fNIRS, sampled from free-ranging cattle. Faecal sampling provides an integrated estimate of the diet selected over the preceding few days, which is more representative of forage quality than either oesophageal fistula or hand-cut forage samples (Coates and Dixon, 2007). Due to the ability of cattle to distinguish green and dead forage (Hendricksen et al., 1982), we contend that NDVI or EVI are suboptimal variables to link with forage quality. Instead, the pixel-wise spectra of satellite imagery should be calibrated to biophysically meaningful components of green cover, dead cover, and bare soil (Scarth et al., 2010; Terrestrial Ecosystem Research Network, 2017).

It would represent a novel advance for grazing management—beyond northern Australia's savannas—to be able to forecast forage quality as related to the temporal dynamics of remotely sensed cover components. A practical difficulty in this pursuit is that forage quality will rarely be measured on the same day as a satellite overpass. This can be an important consideration, due to the variation in forage quality even over short time scales. A further difficulty is creating a framework that yields not only realistic forecasts of forage quality, but also realistic forecasting uncertainty. We propose that these difficulties can be overcome with an appropriately parameterised linear mixed model (Marchant et al., 2009).

The aim of this study was to combine field observations of forage quality with remotely sensed cover components, to develop a linear mixed model that can forecast forage quality for cattle in the dry savannas of northeast Australia. Forecasts were to be made three months ahead of a key decision date, over a 12-year period. We set the date of interest as May 31, a time when the wet season is typically transitioning to the dry, and forage quality can change rapidly. Accurate forecasts, associated with realistic uncertainty, will potentially benefit land managers in northeast Australia, allowing them act in a timely manner.

2. Methods

2.1. Study site

Our study focussed on the long-term cattle-grazing trial at Wambiana station (20°32′24″ S, 146°08′2″ E), in the dry savannas, approximately 50 km south-west of Charters Towers, Queensland, Australia (Fig. 1). Median annual rainfall for Trafalgar Station (17 km from the grazing trial) is 605 mm but 87% of this is typically received between November and March (Bureau of Meteorology, 2021). The site contains three main soil-vegetation communities (with soil nomenclature from International Union of Soil Sciences, Working Group WRB, 2015): *Eucalyptus melanophloia* on Ferralsol soil; an *Acacia harpophylla–Eucalyptus brownii* community on a complex of Ferralsol and Vertisol soil; and *E. brownii* on Solonetz soil. The herbaceous layer consists of a range of native C_4 tropical perennial grasses such as *Aristida* spp., *Bothriochloa ewartiana, Chrysopogon fallax, Dichanthium sericeum,* and various *Digitaria* and *Panicum* species (O'Reagain et al., 2009) as well as various annual species and forbs. The exotic grass *Bothriochloa pertusa* has emerged as a substantial component of pasture since 2007, and the native shrub *Carissa ovata* is particularly associated with the *E. brownii* community.

The trial was conceived to test the ability of different stocking strategies to cope with rainfall variability (O'Reagain et al., 2009). Its longevity—and the volume of data collected—make the trial unique to northern Australia. In 1997 ten contiguous paddocks, all approximately 100 ha, were randomly allocated to one of five grazing treatments (two replicates per treatment; Fig. 1). All paddocks contain similar proportions of the three main soil-vegetation communities. We focussed on the two treatments that have the greatest contrast: (i) moderate stocking rate (MSR), stocked at an average of 9.0 ha per animal equivalent (AE; defined as a 450-kg steer) located in paddocks *A* and *B*; and (ii) heavy stocking rate (HSR), stocked at an average of 6.5 ha per AE in paddocks *C* and *D*. Paddocks are grazed year-round with free-ranging Brahman steers. Following industry practice, animals are supplemented with urea in the dry season and phosphorous in the wet season. In severe droughts, cattle are supplemented with molasses and urea, or removed altogether (O'Reagain et al., 2009).

2.2. Forage quality

We quantified forage quality through two variables: dietary crude protein (DCP) and *in vivo* dry-matter digestibility (DMD). These were estimated by fNIRS, collected from cattle in Paddocks *A–D*, approximately every three weeks between June 1998 and November 2019. For operational reasons, the collection of faecal samples temporarily ceased during October to December 1999, and from June 2011 to January 2012.

Samples were composites, collected from fresh dung pats from at least five animals in each paddock. Faecal samples were air-dried at 60 °C for 48 h, sealed, then stored. Prior to analysis, samples were ground (1-mm screen, Model 1093 Cyclotec mill; Foss Tecator AB, Hoganas, Sweden), redried (65 °C), cooled in a desiccator, then scanned (400–2500-nm range) using a monochromator fitted with a spinning cup module (Foss 6500; NIRSystems, Silver Spring, MD, USA), as described by Coates and Dixon (2011). DCP and DMD were estimated from faecal spectra, using established calibration equations appropriate for the tropical pastures of northern Australia (Dixon and Coates, 2009; Coates and Dixon, 2011).

Faecal samples collected during periods of drought-feeding were

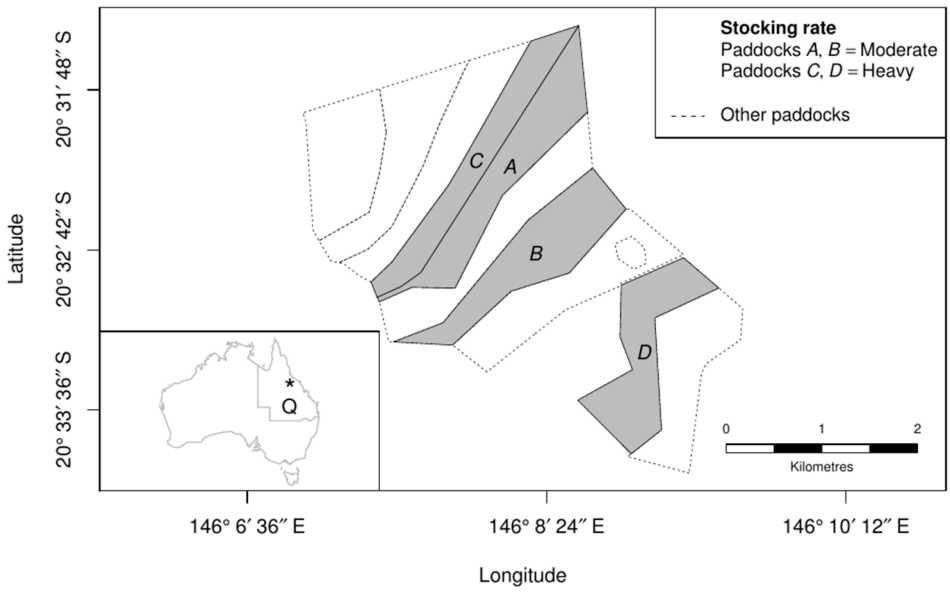

Fig. 1. Layout of the Wambiana grazing trial. Of the ten paddocks available, we consider only Paddocks *A–D* for analysis, which have been under heavy or moderate stocking rates since 1997. Inset: the asterisk shows the location of the trial site relative to the state of Queensland (denoted 'Q'), within Australia.

excluded from the analysis, leaving a total of 1271 faecal samples from the four paddocks. To account for transit through the cattle, we subtracted three days from each sampling date.

2.3. Satellite imagery

Satellite imagery that intersected the study site was collated for the period 1st January 1997 to 29th February 2020, from Landsat-5 TM (Thematic Mapper; images acquired 1997–2011), Landsat-7 ETM+ (Enhanced Thematic Plus; 1999–2020), and Landsat-8 OLI (Operational Land Imager; 2013–2020). Imagery was pre-processed to surface reflectance (Flood et al., 2013). We applied a spectral-unmixing algorithm (Scarth et al., 2010) to every Landsat image, to split pixel-wise surface reflectance into cover proportions of 'bare soil', 'green vegetation', and 'dead (i.e. non-photosynthetic) vegetation'. An in-house algorithm then minimised the influence of tree foliage (thus converting 'green vegetation' to 'green grass'), and simultaneously further split 'dead vegetation' into edible 'dead grass' and inedible 'litter' (see Supplementary Material). Masks were applied to filter undesirable effects from the imagery, e.g. cloud contamination (Zhu et al., 2015), or open water (Fisher et al., 2016). If, following this step, >50% of a paddock's pixels were observed on a particular date—and the paddock was not detected as burnt in the preceding 90 days (Goodwin and Collett, 2014)—then the ratio of paddock-average 'green grass' to 'dead grass' was calculated for further analysis. We herein refer to this variable as GDR.

2.4. A statistical model that forecasts forage quality

We simultaneously modelled DCP, DMD, and GDR, justifiable on the basis that, through their correlation, knowledge of one could help to forecast the other. All three variables are observed irregularly in time. GDR is observed more often than DCP and DMD, but not necessarily on the same day. For simplicity, we first describe the modelling setup as if there were only one response variable—represented generically as z—and then describe extension to the multivariate case.

2.4.1. Basic setup—univariate case

A linear mixed model (LMM) was used to describe the variation of z through time. A LMM splits z into components associated with 'fixed' and 'random' effects: fixed effects describe deterministic responses to given input variables and associated parameters (for instance, a treatment effect that we would like to learn about), while random effects describe probabilistic responses (for instance, a paddock effect that we would like to control for, but are not specifically interested in). The central assumption of the LMM is that the random effects are normally distributed. To this end, we transformed z to natural logarithms prior to fitting. Working backwards from a date of interest, only the 100 most-recent observations of z in each paddock were considered for modelling, and concatenated into a column vector of length $n = 400$:

$$\mathbf{z} = \left[z_{A,1}, \cdots, z_{A,100}, z_{B,1}, \cdots, z_{B,100}, z_{C,1}, \cdots, z_{C,100}, z_{D,1}, \cdots, z_{D,100}\right] \quad (1)$$

where: subscript letters are paddock identifiers, and subscript numbers index the timing of observations, from the newest ('1'), to oldest ('100'). Note that, due to irregular sampling, time '1' of one paddock does not necessarily equal time '1' of another paddock.

The form of the LMM was:

$$\mathbf{z} = \mathbf{X}\boldsymbol{\beta} + \boldsymbol{\varepsilon}_t + \boldsymbol{\varepsilon}_p + \boldsymbol{\varepsilon}_{tp} \quad (2)$$

where: $\mathbf{X}$ was a $n \times q$ design matrix that contained the fixed effects, i.e. values of the q variables with which $\mathbf{z}$ varied linearly; $\boldsymbol{\beta}$ was a length-q vector that contained the parameters that described the relation between $\mathbf{X}$ and $\mathbf{z}$; $\boldsymbol{\varepsilon}_t$ was a length-n vector of random effects that described the time-specific variation of $\mathbf{z}$ (common for all paddocks); $\boldsymbol{\varepsilon}_p$ was a length-n vector of random effects that described the paddock-specific variation of $\mathbf{z}$ (common for all time); and, $\boldsymbol{\varepsilon}_{tp}$ was a length-n vector of random effects that described a time-by-paddock effect on the variation of $\mathbf{z}$. We defined the fixed effects of Eq. (2) in three different ways.

Model 1. Experimental treatments MSR and HSR only, i.e. the dimension of $\mathbf{X}$ was $n \times 2$. The first column of $\mathbf{X}$ was filled wholly with ones; the second column was filled with ones only where the treatment was HSR.

Model 2. Experimental treatments MSR and HSR, and the linear function $\ln(r+1)$, where r was the sum of rain received in the 28 days before a date of interest, averaged from five pluviometers spread across the grazing trial. The dimension of $\mathbf{X}$ was $n \times 3$, i.e. columns 1–2 were as above, and column 3 contained the rain information.

Model 3. Experimental treatments MSR and HSR, plus a cyclic cubic regression spline (Wood, 2017) that was a function of day-of-year, defined with four knots and a period of 365.25 days. The

Box 1
. Procedure to split the dataset for modelling.

Specify the set of years: $Y = \{2008, \cdots, 2019\}$
Choose $y \in Y$
Training
- Make **z** from the 100 most-recent observations of ln(DCP), ln(DMD) and ln(GDR) in each paddock, available to 31 May of y
- Fit a linear mixed model

Forecasting
- Use the linear mixed model to simulate 10,000 forecasts of ln(DCP) and ln(DMD), daily between 1 June and 31 August of y
- Back-transform to DCP and DMD
- Average the simulated daily forecasts by month

dimension of $\mathbf{X}$ was $n \times 4$, i.e. columns 1–2 were as above, and columns 3–4 contained the spline.

We denote as $\boldsymbol{\theta}$ the vector of parameters that describe the random effects in Eq. (2). The time-specific random effects were distributed as $\boldsymbol{\varepsilon}_t \sim \mathcal{N}(0, \mathbf{C}_t)$, where the $n \times n$ covariance matrix $\mathbf{C}_t = \mathbf{R}_t \boldsymbol{\eta}_t \mathbf{R}_t$. Matrix $\boldsymbol{\eta}_t$ is itself the sum of two structures:

$$\boldsymbol{\eta}_t = c_1 f(\mathbf{d}_t) + c_2 g(\mathbf{d}_t, \varphi_t) \tag{3}$$

where: c_1 and c_2 were variance parameters; f was the nugget autocorrelation function; and g was the spherical autocorrelation function (range parameter of φ_t), applied to $\mathbf{d}_t$, the $n \times n$ matrix of absolute time-differences between observations. Following Marchant et al. (2009), $\mathbf{R}_t$ was a $n \times n$ diagonal matrix, with a value of 1.0 when the month of observation was February to October (inclusive), and parameter r_t (where $r_t > 1.0$) elsewhere. This term addressed the non-stationary temporal variance found during exploratory analysis (not shown); in other words, $\mathbf{R}_t$ adjusts variance upward during those months associated with the onset of the wet season.

The paddock-specific random effects were distributed as $\boldsymbol{\varepsilon}_p \sim \mathcal{N}(0, \mathbf{C}_p)$, where $\mathbf{C}_p$ was a $n \times n$ covariance matrix. The element of $\mathbf{C}_p$ at row i and column j was coded as zero, except when the pair of observations was from the same paddock, in which case the element was coded as parameter c_3.

The time-by-paddock random effects were distributed as $\boldsymbol{\varepsilon}_{tp} \sim \mathcal{N}(0, \mathbf{C}_{tp})$, where the $n \times n$ covariance matrix $\mathbf{C}_{tp} = \mathbf{R}_{tp} \boldsymbol{\eta}_{tp} \mathbf{R}_{tp}$. The element of $\boldsymbol{\eta}_{tp}$ at row i and column j was coded as zero, except when the pair of observations was from the same paddock, in which case the element was coded as $c_4 f(d_{ij}) + c_5 g(d_{ij}, \varphi_{tp})$, where c_4 and c_5 were variance parameters, d_{ij} was the absolute time difference between the pair, and φ_{tp} was the range parameter of the spherical autocorrelation function. Matrix $\mathbf{R}_{tp}$ was defined analogously to $\mathbf{R}_t$, where parameter $r_{tp} > 1.0$, depending on the month of observation. Note the constraints that $\mathbf{C}_{tp}$ and:

$$\mathbf{V} = \mathbf{C}_t + \mathbf{C}_p + \mathbf{C}_{tp} \tag{4}$$

must be positive definite, while $\mathbf{C}_t$ and $\mathbf{C}_p$ must be only positive semi-definite.

We optimised $\boldsymbol{\theta} = [c_1, c_2, \cdots, r_t, r_{tp}]^T$ by using the Nelder-Mead simplex (Nelder and Mead, 1965) to maximise the residual log-likelihood function (Patterson and Thompson, 1971), with the aid of scripts custom-written for the R statistical software (R Core Team, 2020). Appropriate values for φ_t and φ_{tp} were pre-determined for each model prior to analysis, based on a grid search, and held constant throughout. The parameters $\boldsymbol{\beta}$ were available analytically for any given combination of values in $\boldsymbol{\theta}$, through generalised least-squares.

The ultimate aim of the modelling was to forecast DCP and DMD. We cycled through the dataset according to the procedure described in Box 1, optimising $\boldsymbol{\theta}$ once per year, based on **z** formed at the end of May, i.e. approximately when land managers in the dry savannas decide what to do with their herd in the coming dry season. Forecasts were made three months ahead, on the basis that they would cover the period when a management decision is essential; little further change in the grazing system is expected between September and the start of the next wet season.

For a year of interest, y, we define the forecasting target $\mathbf{t}_p$ as a length- n_p column vector of days in a forecasting month, e.g. for June $\mathbf{t}_p = [t_1, \cdots, t_{30}]^T$, for an unsampled paddock. We take $\boldsymbol{\theta}$ from y and calculate the empirical best linear unbiased predictor (EBLUP) for **z** at $\mathbf{t}_p$, and its associated covariance matrix, $\mathbf{G}_p$ (Marchant et al., 2009):

$$\hat{\mathbf{z}}(\mathbf{t}_p) = (\mathbf{X}_p - \mathbf{V}_{po}\mathbf{V}^{-1}\mathbf{X})\hat{\boldsymbol{\beta}} + \mathbf{V}_{po}\mathbf{V}^{-1}\mathbf{z} \tag{5}$$

$$\mathbf{G}_p = (\mathbf{X}_p - \mathbf{V}_{po}\mathbf{V}^{-1}\mathbf{X})\mathbf{P}^{-1}(\mathbf{X}_0 - \mathbf{V}_{po}\mathbf{V}^{-1}\mathbf{X})^T + \mathbf{V}_{pp} - \mathbf{V}_{po}\mathbf{V}^{-1}\mathbf{V}_{po}^T \tag{6}$$

where: $\hat{\boldsymbol{\beta}}$ is the vector of estimated fixed effects; $\mathbf{X}$ is the design matrix for the fixed effects at the observation days; $\mathbf{V}$ is from Eq. (4); $\mathbf{X}_p$ is the design matrix for the fixed effects at $\mathbf{t}_p$; $\mathbf{V}_{po}$ is the $n_p \times n$ matrix of covariances between the forecasting target and the data, defined analogously to $\mathbf{V}$; $\mathbf{P} = \mathbf{X}^T\mathbf{V}^{-1}\mathbf{X}$; and, $\mathbf{V}_{pp}$ is the $n_p \times n_p$ matrix of total covariance for the prediction target (i.e. between the forecasting days in the unsampled paddock), defined analogously to $\mathbf{V}$. When forecasting, we ensured conservative values by defining $\mathbf{V}_{po}$ using only the contributions from time-specific covariance (Eq. (3)); the paddock-specific and time-by-paddock covariance terms were set to zero. An advantage of using random effects to model differences between paddocks is that we can learn a more general model about what might happen in other paddocks. Our forecasting setup represents naivety about localised paddock effects, which would be the case if the model were applied outside Wambiana (although such a case would require stringent validation).

While $\hat{\mathbf{z}}(\mathbf{t}_p)$ and $\mathbf{G}_p$ convey all necessary information about a forecast for **z**, they do so at the temporal resolution of a single day. To forecast the monthly mean, we used $\hat{\mathbf{z}}(\mathbf{t}_p)$ and $\mathbf{G}_p$ to simulate 10,000 realisations of correlated multivariate normal deviates. We back-transformed the deviates, then averaged them to create the length-10000 vector **S**. The forecast value for the month was the mean of **S**, and the 95% prediction interval given by its 2.5th and 97.5th percentiles (Fig. 2).

2.4.2. *Extended setup—multivariate case*

We follow Marchant and Lark (2007) and Marchant et al. (2009) in extending a LMM to include DCP, DMD, and GDR as response variables.

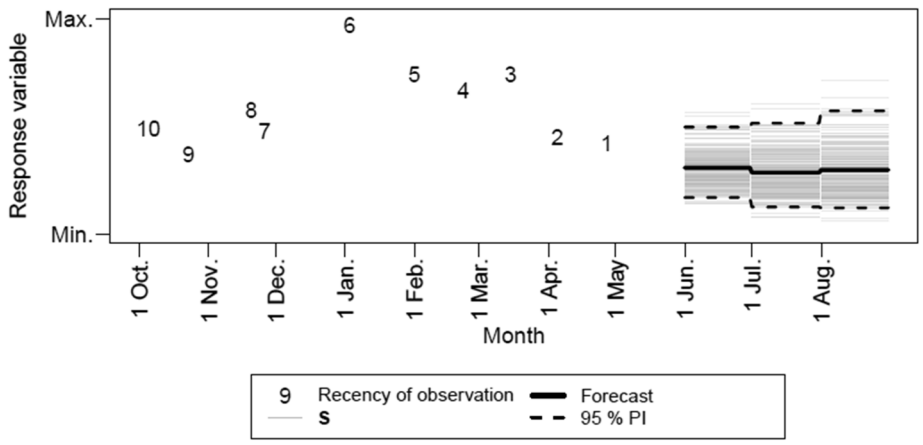

Fig. 2. Forecasting the monthly mean of a response variable, three months ahead from the end of May in a given year. A model is fitted to the 100 most-recent observations of the response variable (only the 10 most recent are shown; note the irregular sampling times). Grey lines are values that comprise the vector **S** (i.e. 10,000 monthly forecasts simulated from the model). The mean value for the forecast and its 95% prediction interval (PI) are obtained from **S**.

In this multivariate case, **z** becomes a concatentation of the response variables, and the dimensions of the remaining terms of Eqs. (2–6) are similarly altered. The most complex aspect of extension concerns the random-effect parameters. These are more numerous in a multivariate case, because it is necessary to account for cross-covariance between each pair of response variables. As in the univariate case, the random-effect parameters must satisfy the condition that $\mathbf{C}_{tp}$ and $\mathbf{V}$ are positive definite, with $\mathbf{C}_t$ and $\mathbf{C}_p$ positive semidefinite. These constraints are pragmatically satisfied by assuming the random effects conform to a linear model of coregionalisation (Marchant and Lark, 2007). In total, the multivariate model has 38 parameters but, for further pragmatism, we only fitted the 15 cross-covariance parameters under the multivariate model; fitted values for auto-covariance parameters and r_t and r_{tp} were inserted from the corresponding univariate models, and held constant.

2.5. Model performance

The splitting procedure in Box 1 created a set of withheld data (i.e. the observations from June to August each year from 2008 to 2019), against which model forecasts could be compared. We assessed the forecasting performance of Models 1–3 for each response variable with: (i) the median absolute error (MAE), where observations in the withheld subset were averaged by month for each paddock, to enable a meaningful comparison; and, (ii) the mean squared deviation ratio (MSDR; Webster and Oliver, 2001):

$$\mathrm{MSDR} = \frac{1}{n_{0,j}} \sum_{i=1}^{n_{0,j}} \left(\frac{\{z_{i,j} - \widehat{z}_{i,j}\}^2}{\widehat{\sigma}^2_{i,j}} \right) \tag{7}$$

where: $n_{0,j}$ was the number of withheld observations associated with the j^{th} response variable; $z_{i,j}$ was the i^{th} withheld log-transformed observation; $\widehat{z}_{i,j}$ was the corresponding log-transformed forecast; and, $\widehat{\sigma}^2_{i,j}$ was the corresponding prediction variance, from Eq. (6). For MAE, the smaller the value, the better the model. The log-normal nature of the response variables meant that a conventional measure of model performance, e.g., root-mean-square-error might be impacted by a small number of large prediction errors. MAE is less dominated by these errors and is preferred here. MSDR is used to assess the goodness-of-fit of the model parameters: the target value of 1.0 indicates that the prediction uncertainty is realistic, and that, by extension, the optimised random-effect parameters are appropriate for the data.

3. Results

3.1. Exploratory analysis

The observations of DCP, DMD, and the four cover proportions show prominent seasonality (Fig. 3). Peaks in the time-series of DCP and DMD and green grass tended to have a shorter duration than troughs, reflecting the relatively long dry season that is typical of dry savannas. Note that the density of the cover observations decreased in periods when there was only one Landsat satellite available, i.e. prior to 2003, and 2010–2012.

The three log-transformed response variables were positively correlated, as expected (Table 1), i.e. as the observations of one variable increased, the others tended to increase too, and *vice versa*. In regard to the potential utility of remote sensing, GDR had a stronger correlation with forage quality than NDVI. The distributions of the log-transformed response variables were approximately normal (not shown).

3.2. Model diagnostics

Over the 12 years of analysis, the mean length of time covered by the 100 most-recent observations was 7.4 years for DCP and DMD, and 4.5 years for GDR. These lengths reflect the approximately three-weekly sampling interval of DCP and DMD at Wambiana, and the (at best) 8-day sampling interval for GDR.

For all years, treatments and paddocks, we judged Model 3 to give the most reliable forecasts of the response variables (Table 2). Compared with Models 1 and 2, Model 3 is associated with the smallest values of MAE. Given the data-range of each forage-quality variable (DCP = 2.1–16.1%, DMD = 45.0–70.4%; Fig. 3), DMD was forecast with better relative accuracy than DCP. For MSDR, Model 1 consistently overestimated the forecasting uncertainty of the response variables. And while Model 2 gave realistic forecasting uncertainties for DCP and DMD, GDR was poorly represented. Model 3 underestimated the forecasting uncertainties for DCP and GDR to about the same extent that it overestimated that for DMD. The MSDR values for Model 3 are further from 1.0 than desired, and suggest that some parameters were not completely optimised. This is not surprising given: (i) the pragmatic way that we fitted the 38 parameters of the model, joining univariate optimisations with multivariate; and, (ii) applying MSDR in a forecasting framework is a relatively harsh test, because the model is extrapolating, not interpolating.

We investigated Model 3 further. Optimum values of the range parameters, found by a preliminary grid search then held constant over all years, were $\varphi_t = \varphi_{tp} = 182.6$ days. Over all years, the average amount of

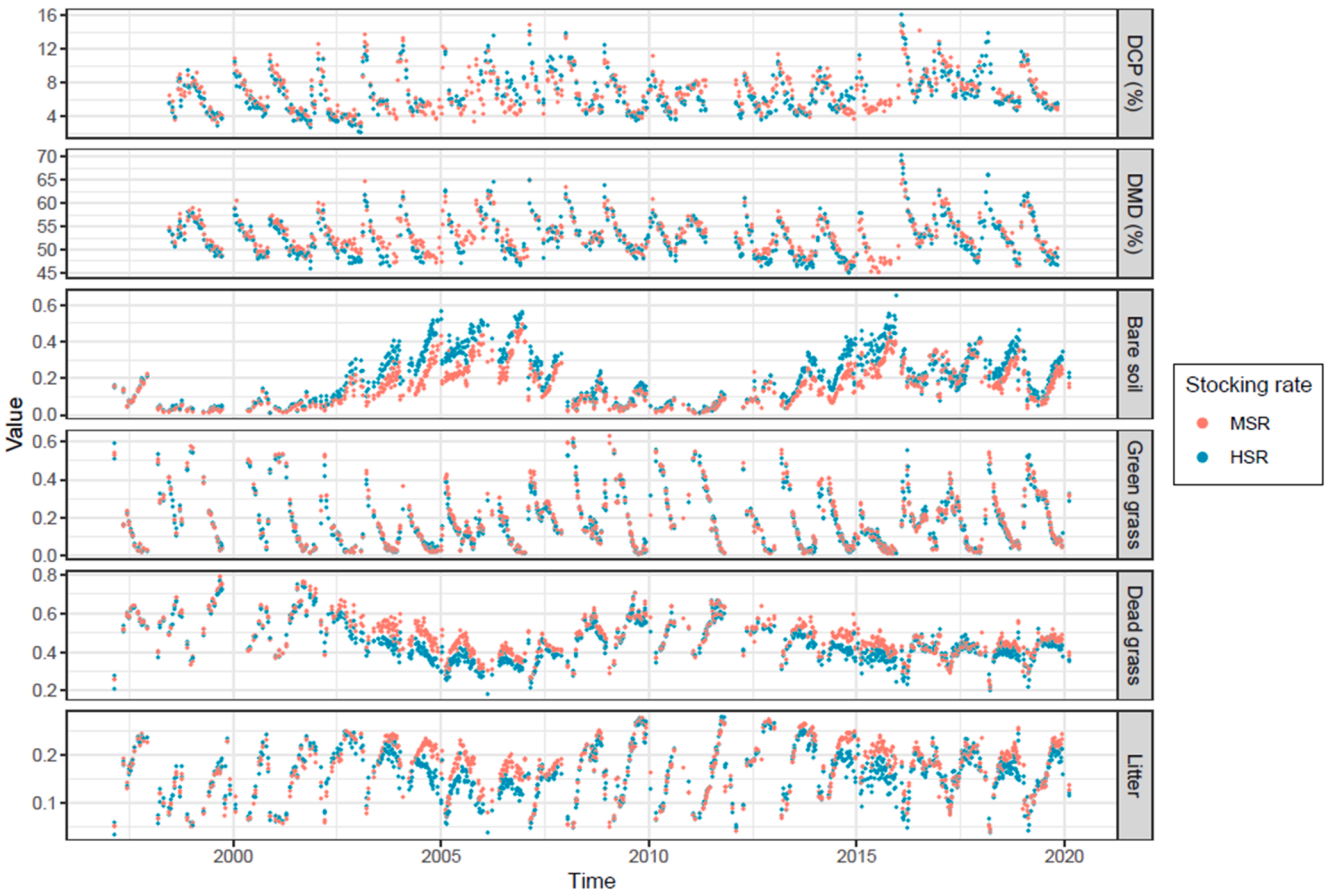

Fig. 3. Observations of relevant variables through time, coloured by stocking rate (MSR = moderate; HSR = heavy).

Table 1
Pearson correlation coefficients of the log-transformed response variables. Log-transformed NDVI is included for comparative purposes. Results have been pooled over paddocks and years.

	ln(DMD)	ln(GDR)	ln(NDVI)
ln(DCP)	0.79	0.65	0.54
ln(DMD)		0.63	0.56
ln(GDR)			0.82

Table 2
MAE (median absolute error) and MSDR (mean squared deviation ratio) when forecasting up to three months ahead from the end of May. Results have been pooled over paddocks, forecasting months, and years. Note that MSDR applies to values of the log-transformed response variable.

	MAE			MSDR		
Response variable	Model 1	Model 2	Model 3	Model 1	Model 2	Model 3
DCP (%)	1.17	1.49	0.86	0.83	0.96	1.28
DMD (%)	1.83	2.07	0.95	0.69	0.94	0.71
GDR	0.21	0.25	0.07	0.46	0.45	1.31

variance explained by the fixed effects, $\mathbf{X}\hat{\boldsymbol{\beta}}$, was 40% for ln(DCP), 56% for ln(DMD), and 49% for ln(GDR). In comparison with Model 1—where the corresponding values were all $\leq 1\%$—the cyclic cubic splines were a key inclusion, enabling Model 3 to capture a substantial amount of the response variables' seasonality, which in turn yielded more sensible values in $\boldsymbol{\theta}$, especially in regard to GDR. When forecasting three months ahead from the end of May, the model reproduced some of the observed correlation of DCP with DMD (Fig. 4), but non-linearity meant that the five largest values of DCP were not well predicted. Three of these five values were from the winter of 2016, which was atypical for two reasons. First, a large outlying observation of DCP collected in early July was associated with a sample that contained an unusually large proportion of non-grass, suggesting that the cattle had found a localised patch of legumes or forbs. Second, there was a 90-mm downpour on 18 July that followed a run of relatively dry summers. This out-of-season rain provided a burst of new plant growth and DCP for the cattle, as grasses were suddenly able to access the mineral N that had been accumulating in the soil.

The inclusion of experimental treatments MSR and HSR in the fixed effects of Model 3 enables a test of the null hypothesis that forage quality is unaffected by stocking rate (Table 3). Over all years, DMD was more sensitive to stocking rate than DCP, with DMD tending to be significantly lower under heavy stocking rates. The strength of the stocking-rate effect from year to year was associated with summer rainfall, being greater in the run of relatively dry years from 2013 onward. This implies that utilisation rate (i.e. the ratio of pasture eaten to pasture grown) is important for determining forage quality.

It is illuminating to see the forecasts of Model 3 compared with corresponding observations as a function of time (Fig. 5). According to the procedure in Box 1, each year is associated with a different set of fitted parameters, and data collected after May 31 are withheld. The monthly forecasts are reasonably accurate in most years, with all three response variables generally declining, as expected, as each winter progressed. Prediction uncertainty increased with each passing month, which was also an expected result. The summer of 2014–2015 was especially dry (Table 3), so forage quality in the post-growth period was particularly poor. As noted above, the winter of 2016 was atypical, so the forecasts and observations diverged strongly.

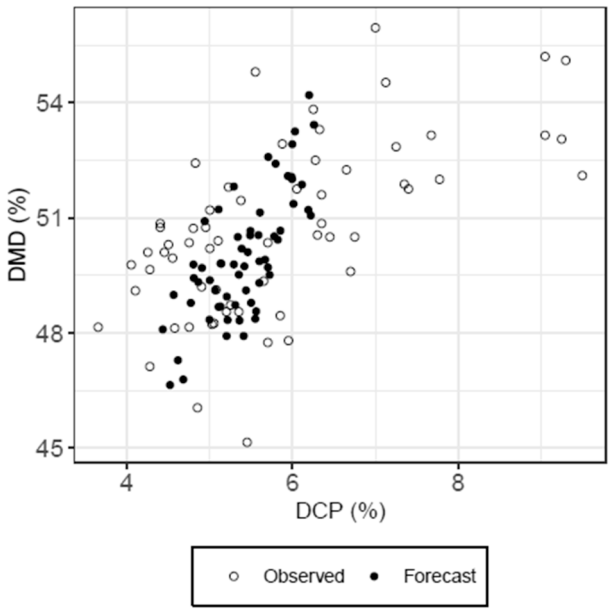

Fig. 4. Monthly-averaged observations and forecasts of Model 3 for DCP and DMD for June–August, pooled over years and paddocks.

4. Discussion

4.1. Implications for cattle management

To the best of our knowledge, our study is the first to successfully link forage quality for cattle with remotely sensed groundcover information, over a > 20-year period. Previous research at the Wambiana grazing trial has linked forage *quantity*, in the form of total standing dry matter, with remotely sensed information (Schmidt et al., 2016), but did not examine forage quality. The results of our study suggest that, in a southern hemisphere dry savanna that is dominated by C_4 grassland, it is possible to forecast monthly-average forage quality ahead from the end of the summer wet season (approximately May) into the first three months of the winter dry season, albeit with increasing uncertainty. The end of the wet season is a critical time of year, when early management intervention can prevent future losses in animal production.

A number of previous studies have related forage quality to remotely sensed information: some from faecal sampling (Ryan et al., 2012; Villamuelas et al., 2016; Tolleson et al., 2020); some with forage quality determined from less-desirable hand-clipped samples (Phillips et al., 2009; Zengeya et al., 2013; Ferner et al., 2015; Barnetson et al., 2020). Of these studies, the period of forage-quality sampling was, at most, five years. While Geremia et al. (2019) tracked pasture green-up with satellite data over 16 years, actual forage quality was only measured in a single five-month period. Possibly the longest study is that of Creech et al. (2016), who tracked diet quality estimated from faecal N in desert bighorn sheep over an 11-year period. In comparison, our study is based on 23 years of forage-quality data, collected from cattle faeces at approximately 3-week intervals. In regard to remote sensing, our analysis was driven by the variable GDR, defined as the cover ratio of 'green grass' to 'dead grass'. GDR had a stronger correlation with forage quality than the conventional NDVI (Table 1), and makes biological sense given that cattle select for green, rather than dead, forage (Hendricksen et al., 1982). Furthermore, by correcting for leaf-litter (see Supplementary Material), we hope that our Landsat-based GDR values can be robustly extrapolated to different landscapes. A disadvantage of Landsat is that it does not sense in the red-edge of the electromagnetic spectrum, which has been shown to correlate with forage quality (Barnetson et al., 2020). This suggests a future role for Sentinel-2 satellites, which, in contrast to Landsat, sense with four red-edge bands (sentinels.copernicus.eu/web/sentinel/missions/sentinel-2).

We have shown that forage quality, particularly DMD, tended to be significantly lower under heavy stocking (Table 3), although this was dependent on rainfall. The HSR treatment has become associated with a scarcity of palatable perennial species, due to overgrazing. The lower quality diet of cattle in the HSR treatment leads to reduced liveweight gain (O'Reagain et al., 2018). However, in years with well-distributed rainfall, the constant supply of short-lived, green regrowth in the HSR treatment allows cattle to select a diet that is, at least in terms of DCP, of relative high quality.

There is a demand for decision-support tools that assist land managers in the extensive grazing enterprises of northeast Australia to make more frequent, better-informed decisions (McCartney, 2017; Paxton, 2019). Following appropriate testing at other sites, we ultimately anticipate packaging forecasts of forage quality as a simple graphical product (Fig. 6). In May of a year of interest, the product would be available on request for a particular paddock, delineated by the user. The optimised parameters of Model 3 would then be combined with the 100 most-recent local observations of GDR and user-provided DCP or DMD. Predictions for May (the 'nowcast') and forecasts for June to August would be returned. Included in this product is the ratio of protein to metabolisable energy:

$$H = (10.0 \times \mathrm{DCP})/(0.17 \times \mathrm{DMD} - 2.0) \quad (8)$$

which has units of g MJ^{-1}. The denominator of Eq. (8) is taken from Standing Committee on Agriculture, Ruminants Subcommittee, 1990, p.9). A separate model is not needed to estimate H ; its distribution is found by simply plugging in the simulated daily predictions for DCP and DMD, then averaging by month, as in Fig. 2. We follow Dixon and Coates (2010) and set 6% as a general threshold for DCP less than the requirement for cattle maintenance, but acknowledge that operationally the value depends on factors such as the class of cattle and the target market. In the example in Fig. 6, it is apparent that the forecast is less-than-desirable.

A graphical product such as Fig. 6 could, when combined with other sources of information such as seasonal forecasts of ground cover (e.g. www.longpaddock.qld.gov.au), prompt a land manager to intervene with supplementation, or to perhaps reduce the number of animals held. Such a system would be an advance on the conventional industry practice, where forage quality is acknowledged to be crucial to cattle production but is difficult to monitor. May is an important period for land managers in northern Australia, but our analysis is not restricted to

Table 3

The estimated fixed-effect parameter, $\widehat{\boldsymbol{\beta}}$, in Model 3 that corresponded to the effect of the high stocking-rate treatment (HSR) on ln(DCP) and ln(DMD), relative to moderate stocking rate. Tests of significance were done on the log-transformed scale ($^{+} = P < 0.1$; $* = P < 0.05$; $** = P < 0.01$), but for convenience $\widehat{\boldsymbol{\beta}}$ has been back-transformed to represent a multiplicative effect, i.e. a value < 1 indicates HSR proportionately decreased the response variable, and *vice versa*. Summer rain is accumulated between November (of the previous year) and March, based on pluviometers located across the study site.

	$\exp(\widehat{\boldsymbol{\beta}})$		
Year	DCP	DMD	Summer rain (mm)
2008	1.039	0.978**	998
2009	1.040	0.982*	665
2010	1.046	0.986^{+}	768
2011	1.028	0.987	666
2012	1.007	0.985^{+}	703
2013	0.958	0.984*	352
2014	0.917**	0.986*	450
2015	0.928**	0.984*	215
2016	0.927**	0.985**	410
2017	0.934**	0.986*	344
2018	0.965	0.985**	509
2019	0.973	0.990^{+}	462

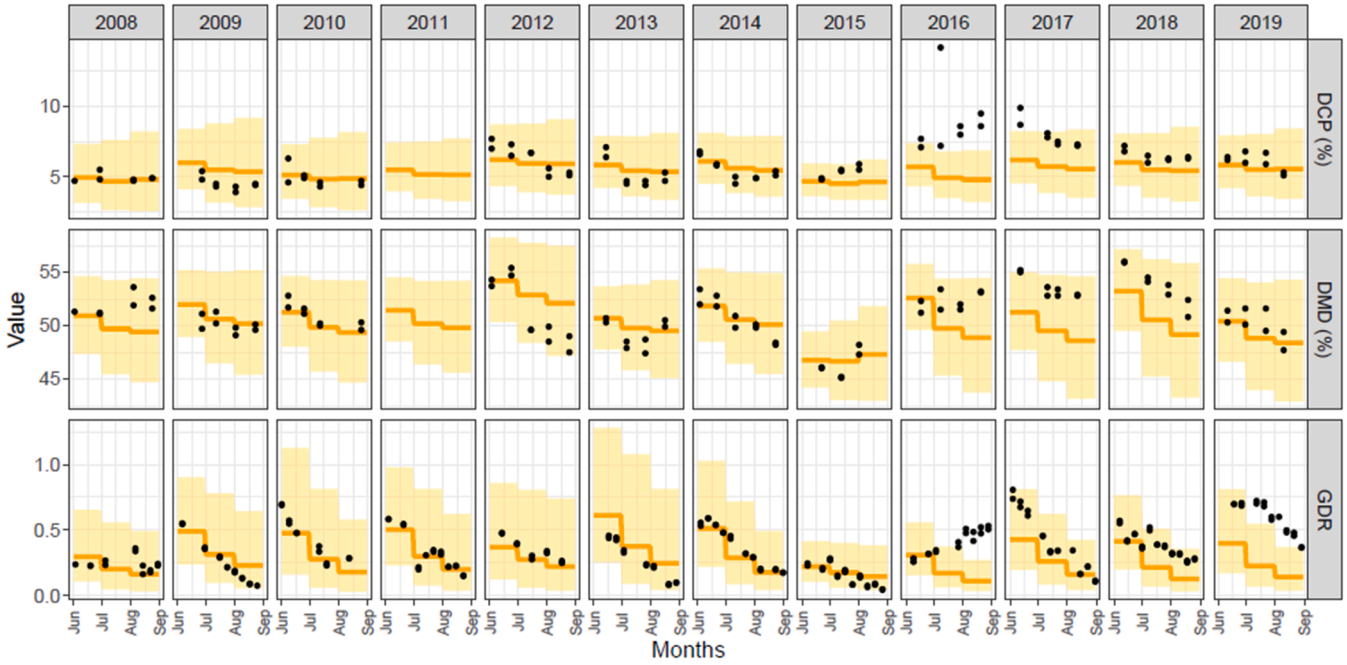

Fig. 5. Monthly forecasts of the response variables for each winter of each year, for the moderate stocking rate (MSR) treatment. The orange line is the predicted mean; the yellow region is the 95% prediction interval. For comparison, observed daily values are also presented. MSR paddocks were destocked for the winter of 2011, so no observations of forage quality were made. (For interpretation of the references to colour in this figure legend, the reader is referred to the web version of this article.)

that month alone; it could conceivably be run each month continuously, over the landscape as new Landsat imagery is acquired. Ultimately, we aim to forecast not just forage quality, but animal liveweight gain. The data to support such an advance are currently too limited.

4.2. Model calibration and behaviour

The cyclic cubic regression spline used as a fixed-effect in Model 3 adequately captured the seasonal behaviour of DCP, DMD, and GDR. When this seasonality was combined with coregionalised random effects, the result was the most reliable of the models investigated, able to forecast with a MAE of 0.86% for DCP and 0.95% for DMD (Table 2). Model 1 was naïve about the recent behaviour of the green signal, so its forecasting accuracy suffered. Despite the inclusion of information about recent rainfall as an explanatory variable, Model 2 performed even worse than Model 1 in terms of MAE, which suggests that recent rainfall at Wambiana is no indicator of future rainfall. The uncertainty of the forecasts, summarised by MSDR in Table 2, was difficult to realistically represent, especially for GDR in Model 1 and Model 2. Note that, to fit the various models, DCP, DMD, and GDR did not have to be temporally coincident, nor did we have to introduce spurious uncertainties into the workflow by *ad hoc* interpolation to common days.

We pragmatically specified that only the 100 most-recent observations of DCP, DMD, and GDR were used for fitting and forecasting the model in each year. The number could be increased, but at an exponential cost to the computing time. The (at best) 8-day sampling interval between overpasses of Landsat satellites meant that 4.5 years were needed, on average, to accumulate the 100 most-recent observations of GDR. If another source of satellite imagery were added into the mix—e.g. Sentinel-2, with its (at best) 5-day temporal resolution—then the 4.5 years would reduce greatly, with the resultant GDR time-series possibly becoming too short to detect seasonal variability. For further pragmatism we also combined the optimised parameter values of both univariate and multivariate runs of the LMM.

Given that fNIRS is not routinely conducted on all cattle properties, the prediction intervals shown in Fig. 5 are probably best-case scenarios. However, consistent Landsat coverage means that all grazing properties in northeast Australia will always have available the 100 most-recent observations of GDR. Thus, if applying our model to a new area, the typical case will be for few observations of DCP and DMD (perhaps even just a single approximate mean for each), and the full quota of GDR observations. This exemplifies the 'undersampling' scenario discussed by Webster and Oliver (2001, p. 206) where multivariate modelling brings benefit over univariate modelling: because correlations are explicitly parameterised, the densely sampled variable will guide the predicted values of a sparsely sampled variable, and do so with greater precision than a univariate method. Model performance in this situation will, however, require rigorous testing.

Four aspects of this study require further exploration. First, we need to incorporate into the model the forage-quality and GDR data from other short-term grazing studies in Australia, e.g. Burrows et al. (2010). Second, to forecast robustly over a very large area, the model will inevitably need to consider climate and soil information as explanatory variables. Tolleson et al. (2020) demonstrated, for example, the utility of growing degree days for predicting forage quality, but we speculate that it may have limited applicability in Australia due to the sparsity of weather stations in rural areas. Third, greater explanatory power at the paddock scale may be achieved by relating forage quality to a weighted function of greenness at the scale of a Landsat pixel. Such an idea might help to streamline the number of random-effect parameters, because the remote sensing information would be used as an explanatory, rather than a response, variable. Finally, we have not yet considered how to deal with local outliers, such as the unusually large DCP datum collected in the winter of 2016 (Fig. 5).

An ultimate limit on forecasting accuracy might well be the error inherent in the fNIRS calibrations relative to wet chemistry, with typical standard errors of cross-validation of 0.9–1.5% for DCP, and 1.1–3.2% for DMD (Dixon and Coates, 2009). As the calibrations improve, so too will our model. Regardless of the form of the model, accurate forecasting of DCP and DMD, guided by GDR, will always be challenging, because it effectively involves calibrating a mass-based quantity from a cover-based quantity, which is a strongly non-linear and complex relation

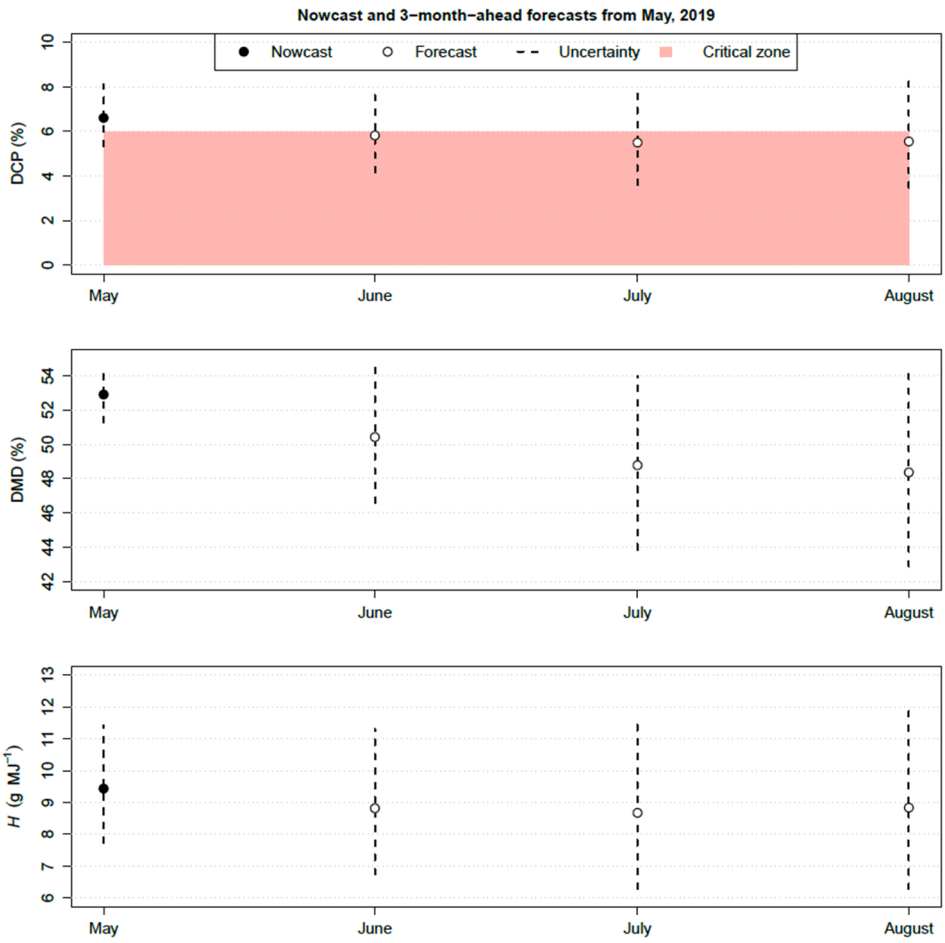

Fig. 6. A prototype summary of results for an individual paddock, representing: the 'nowcast' at the end of May (current status); forecasts for the three following months; and the critical zone (coloured), within which animal nutrition will decline. This example is for the study site at the end May in 2019, assuming that stocking rates are moderate. DCP = digestible crude protein; DMD = *in vivo* dry-matter digestibility; H = ratio of protein to metabolizable energy (Eq. (8)).

(Carter et al., 2015).

4.3. Model assumptions and alternatives

As is necessary for any statistical modelling, we invoked a number of assumptions for this study. The first was that fNIRS indicates what cattle have eaten three days before. Three days reasonably approximates the mean retention time of 65 h reported for cattle (Bartocci et al., 1997), but the same study also found that retention time could be as little as 19 h. Retention time is partly a function forage quality; it may be possible to explicitly incorporate this effect into the modelling, but it would introduce a number of further assumptions, e.g. animal breed, age, and pregnancy.

The assumptions that underly the multivariate LMM are quite stringent. The random effects of the LMM must be normally distributed (which we tried to satisfy with transformation to natural logarithms), and also conform to a coregionalisation (which determines how the random-effect parameters are constrained, to ensure positive definite covariance; Marchant and Lark, 2007). As a result of the coregionalisation, ln(DCP) and ln(DMD) were linearly correlated; upon back-transformation, some non-linearity in the correlation was evident, which agrees with the finding of Lukas et al. (2005). Non-linearity meant that our model could not forecast well the largest values of DCP in winter (Fig. 4). Furthermore, temporal variation was modelled by a spherical autocorrelation function. The φ parameter of the two spherical functions of Model 3 (see Eq. (3)) meant that there was no correlation between observations more than six months apart. A periodic correlation function would be more biologically sensible (Pringle, 2013), but would not enable the use of sparse matrices, whose computational efficiency will help to scale the model-fitting procedure as the dataset inevitably grows. Eventually, the dataset may grow to a point where we need to seek an alternative to a coregionalisation-based model anyway, e.g. the kernel convolution approach (Fanshawe and Diggle, 2012).

Related to assumptions around parameterisation is our use of the Nelder-Mead simplex (Nelder and Mead, 1965) to minimise the residual log-likelihood function. Simulated annealing is an alternative method for the linear model of coregionalisation (Lark and Papritz, 2003), but in our opinion is too slow to converge. Further alternatives may lie in particle swarm optimisation (Freitas et al., 2020), or perhaps a more sophisticated optimisation/interpretation framework such as the PEST ('parameter estimation') software suite (Doherty, 2015).

5. Conclusion

Cattle production in the dry savannas of northern Australia conventionally relies on a combination of experience, intuition, and hope. In this region, the quality of forage is held to be as important as forage quantity. At the end of the summer wet season each year, typically in May, land managers must make a decision about what to do with their stock in the coming winter dry season: sell, move, or supplement. In this study we have proposed a decision-support tool for land managers, where a statistical model is used to forecast forage quality—defined by dietary crude protein and dry-matter digestibility—as

monthly-average values for the period June to August. The uncertainty of each forecast value is explicitly acknowledged, which is an honest admission of our model's imperfections, and helps the user ultimately set their own thresholds for action.

To the best of our knowledge, our study is the first to link > 20 years of on-ground measurements of forage quality for cattle with the information derived from satellite imagery. The remote sensing-based information used was the ratio of 'green grass' cover to 'dead (i.e. non-photosynthetic) grass' cover, derived from an archive of Landsat surface-reflectance imagery. Dietary crude protein was forecast with a median absolute error (MAE) of 0.86%; dry-matter digestibility was forecast with MAE = 0.95%. Model forecasts were generally consistent over a 12-year validation period, but broke down if there was atypical winter rain.

Two particularly difficult aspects of the study that we overcame were: (i) how forage-quality measurements were rarely coincident with a satellite overpass; and, (2) how to pragmatically manage computational loads when fitting the model. Future research will involve testing the current model at more locations and investigating alternative explanatory variables for the model.

CRediT authorship contribution statement

M.J. Pringle: Conceptualization, Methodology, Software, Formal analysis, Investigation, Data curation, Visualization, Writing – original draft, Writing – review & editing. **P.J. O'Reagain:** Conceptualization, Methodology, Investigation, Resources, Data curation, Writing – original draft, Writing – review & editing, Supervision, Project administration. **G.S. Stone:** Conceptualization, Writing – original draft, Writing – review & editing. **J.O. Carter:** Conceptualization, Methodology, Writing – original draft, Writing – review & editing, Supervision. **T.G. Orton:** Methodology, Software, Writing – original draft, Writing – review & editing. **J.J. Bushell:** Conceptualization, Investigation, Resources, Data curation, Project administration.

Declaration of Competing Interest

The authors declare that they have no known competing financial interests or personal relationships that could have appeared to influence the work reported in this paper.

Acknowledgements

This project was funded by Meat and Livestock Australia (B. ERM.0108). We are grateful to the Lyons family of 'Wambiana' and the Wambiana Grazier Advisory Committee for their continued interest, guidance, and support in running the experiment. The Wambiana grazing trial is co-funded by the Queensland Department of Agriculture and Fisheries, and Meat and Livestock Australia. We thank Peter Allen, Chris Holloway and other colleagues for their help running the trial and collecting faecal samples. Thanks also to Rob Dixon and David Mayer for comments on an early draft.

Appendix A. Supplementary data

Supplementary data to this article can be found online at https://doi.org/10.1016/j.ecolind.2021.108426.

References

Barnetson, J., Phinn, S., Scarth, P., 2020. Estimating plant pasture biomass and quality from UAV imaging across Queensland's rangelands. AgriEngineering 2, 523–543. https://doi.org/10.3390/agriengineering2040035.

Bartocci, S., Amici, A., Verna, M., Terramoccia, S., Martillotti, F., 1997. Solid and fluid passage rate in buffalo, cattle and sheep fed diets with different forage to concentrate ratios. Livest. Prod. Sci. 52 (3), 201–208. https://doi.org/10.1016/S0301-6226(97)00132-2.

Burrows, W.H., Orr, D.M., Hendricksen, R.E., Rutherford, M.T., Myles, D.J., Back, P.V., Gowen, R., 2010. Impacts of grazing management options on pasture and animal productivity in a *Heteropogon contortus* (black speargrass) pasture in central Queensland. 4. Anim. Prod. Sci. 50, 284–292. https://doi.org/10.1071/AN09145.

Callaghan, M.J., Tomkins, N.W., Benu, I., Parker, A.J., 2014. How feasible is it to replace urea with nitrates to mitigate greenhouse gas emissions from extensively managed beef cattle? Anim. Prod. Sci. 54, 1300–1304. https://doi.org/10.1071/AN14270.

Campbell, H.A., Loewensteiner, D.A., Murphy, B.P., Pittard, S., McMahon, C.R., 2021. Seasonal movements and site utilisation by Asian water buffalo (*Bubalus bubalis*) in tropical savannas and floodplains of northern Australia. Wildlife Res. 48, 230–239. https://doi.org/10.1071/WR20070.

Terrestrial Ecosystem Research Network, 2017. Fractional cover. URL: www.auscover.org.au/datasets/fractional_cover (accessed 23 November 2021).

Bureau of Meteorology, 2021. Monthly rainfall: Trafalgar Station. URL: http://www.bom.gov.au/jsp/ncc/cdio/wData/wdata?p_nccObsCode=139&p_display_type=dataFile&p_stn_num=034010 (accessed 23 November 2021).

Carter, J., Stone, G., Trevithick, R., O'Reagain, P., Phelps, D., Cowley, R., Pringle, M., Scanlan, J., Hoffman, M., 2015. Estimating Pasture Total Standing Biomass (TSDM) From Landsat Fractional Cover, Final Report—Volume 2, Project ERM.0098 Meat and Livestock Australia Limited 2015 North Sydney, Australia. URL www.mla.com.au/contentassets/17a4e655dc934f02814e17e143ab861f/b.erm.0098_final_report_2_.pdf (accessed 23 November 2021).

Coates, D.B., Dixon, R.M., 2007. Faecal near infrared reflectance spectroscopy (F.NIRS) measurements of non-grass proportions in the diet of cattle grazing tropical rangelands. Rangeland J. 29, 51–63. https://doi.org/10.1071/RJ07011.

Coates, D.B., Dixon, R.M., 2011. Developing robust faecal near infrared spectroscopy calibrations to predict diet dry matter digestibility in cattle consuming tropical forages. J. Near Infrared Spec. 19 (6), 507–519. https://doi.org/10.1255/jnirs.967.

Creech, T.G., Epps, C.W., Monello, R.J., Wehausen, J.D., 2016. Predicting diet quality and genetic diversity of a desert-adapted ungulate with NDVI. J. Arid Environ. 127, 160–170. https://doi.org/10.1016/j.jaridenv.2015.11.011.

Dixon, R., Coates, D., 2009. Near infrared spectroscopy of faeces to evaluate the nutrition and physiology of herbivores. J. Near Infrared Spec. 17, 1–31. https://doi.org/10.1255/jnirs.822.

Dixon, R.M., Coates, D.B., 2010. Diet quality estimated with faecal near infrared reflectance spectroscopy and responses to N supplementation by cattle grazing buffel grass pastures. Anim. Feed Sci. Technol. 158 (3-4), 115–125. https://doi.org/10.1016/j.anifeedsci.2010.04.002.

Doherty, J., 2015. Calibration and Uncertainty Analysis for Complex Environmental Models. Watermark Numerical Computing, Brisbane, Australia.

Fanshawe, T.R., Diggle, P.J., 2012. Bivariate geostatistical modelling: a review and an application to spatial variation in radon concentrations. Environ. Ecol. Stat. 19 (2), 139–160. https://doi.org/10.1007/s10651-011-0179-7.

Ferner, J., Linstädter, A., Südekum, K.-H., Schmidtlein, S., 2015. Spectral indicators of forage quality in West Africa's tropical savannas. Int. J. Appl. Earth Obs. 41, 99–106. https://doi.org/10.1016/j.jag.2015.04.019.

Fisher, A., Flood, N., Danaher, T., 2016. Comparing landsat water index methods for automated water classification in eastern Australia. Remote Sens. Environ. 175, 167–182. https://doi.org/10.1016/j.rse.2015.12.055.

Flood, N., Danaher, T., Gill, T., Gillingham, S., 2013. An operational scheme for deriving standardised surface reflectance from Landsat TM/ETM+ and SPOT HRG imagery for eastern Australia. Remote Sens. 5, 83–109. https://doi.org/10.3390/rs5010083.

Fordyce, G., Anderson, A., McCosker, K., Williams, P.J., Holroyd, R.G., Corbet, N.J., Sullivan, M.S., 2013. Liveweight prediction from hip height, condition score, fetal age and breed in tropical female cattle. Anim. Prod. Sci. 53, 275–282. https://doi.org/10.1071/AN12253.

Freitas, D., Guerreiro Lopes, L., Morgado-Dias, F., 2020. Particle swarm optimisation: a historical review up to the current developments. Entropy 22, 362. https://doi.org/10.3390/e22030362.

Geremia, C., Merkle, J.A., Eacker, D.R., Wallen, R.L., White, P.J., Hebblewhite, M., Kauffman, M.J., 2019. Migrating bison engineer the green wave. Proc. Natl Acad. Sci. U.S.A. 116 (51), 25707–25713. https://doi.org/10.1073/pnas.1913783116.

Goodwin, N.R., Collett, L.J., 2014. Development of an automated method for mapping fire history captured in Landsat TM and ETM+ time series across Queensland, Australia. Remote Sens. Environ. 148, 206–221. https://doi.org/10.1016/j.rse.2014.03.021.

Hendricksen, R., Rickert, K.G., Ash, A.J., McKeon, G.M., 1982. Beef production model. In: Animal Production in Australia: Proceedings of the Australian Society of Animal Production. Pergamon Press (Australia) Pty Ltd, pp. 204–208.

Huete, A., Didan, K., Miura, T., Rodriguez, E.P., Gao, X., Ferreira, L.G., 2002. Overview of the radiometric and biophysical performance of the MODIS vegetation indices. Remote Sens. Environ. 83 (1-2), 195–213. https://doi.org/10.1016/S0034-4257(02)00096-2.

Lark, R.M., Papritz, A., 2003. Fitting a linear model of coregionalization for soil properties using simulating annealing. Geoderma 115, 245–260. https://doi.org/10.1016/S0016-7061(03)00065-X.

Lukas, M., Südekum, K.-H., Rave, G., Friedel, K., Susenbeth, A., 2005. Relationship between fecal crude protein concentration and diet organic matter digestibility in cattle. J. Anim. Sci. 83, 1332–1344. https://doi.org/10.2527/2005.8361332x.

Marchant, B.P., Lark, R.M., 2007. Estimation of linear models of coregionalization by residual maximum likelihood. Eur. J. Soil Sci. 58 (6), 1506–1513. https://doi.org/10.1111/j.1365-2389.2007.00957.x.

Marchant, B.P., Newman, S., Corstanje, R., Reddy, K.R., Osborne, T.Z., Lark, R.M., 2009. Spatial monitoring of a non-stationary soil property: phosphorus in a Florida water conservation area. Eur. J. Soil Sci. 60, 757–769. https://doi.org/10.1111/j.1365-2389.2009.01158.x.

International Union of Soil Sciences, Working Group WRB, 2015. World Reference Base for Soil Resources 2014, update 2015: International soil classification system for naming soils and creating legends for soil maps. World Soil Resources Reports No. 106. FAO, Rome. URL: www.fao.org/3/i3794en/I3794EN.pdf (accessed 23 November 2021).

McCartney, F., 2017. Factors Limiting Decision Making for Improved Drought Preparedness and Management in Queensland Grazing Enterprises: Rural Specialists' Perspectives and Suggestions. Department of Science, Information Technology and Innovation, Brisbane, Australia. URL: data.longpaddock.qld.gov.au/static/dcap/DCAP1+Social+Science+Final+Report.pdf (accessed 23 November 2021).

McCown, R.L., 1981. The climatic potential for beef cattle production in tropical Australia: Part I—Simulating the annual cycle of liveweight change. Agric. Syst. 6 (4), 303–317. https://doi.org/10.1016/0308-521X(81)90065-2.

McIvor, J.G., 1981. Seasonal changes in the growth, dry matter distribution and herbage quality of three native grasses in northern Queensland. Aust. J. Exp. Agr. Anim. Husb. 21, 600–609. https://doi.org/10.1071/EA9810600.

McKeon, G., Stone, G., Ahrens, D., Carter, J., Cobon, D., Irvine, S., Syktus, J., 2021. Queensland's multi-year Wet and Dry periods: implications for grazing enterprises and land resources. Rangeland J. 43, 121–142. https://doi.org/10.1071/RJ20089.

Nelder, J.A., Mead, R., 1965. A simplex method for function minimization. Comput. J. 7 (4), 308–313. https://doi.org/10.1093/comjnl/7.4.308.

Norman, M.J.T., 1965. Seasonal performance of beef cattle on native pasture at Katherine, N.T. Aust. J. Exp. Agr. 5, 227–231. https://doi.org/10.1071/EA9650227.

O'Reagain, P., Bushell, J., Holloway, C., Reid, A., 2009. Managing for rainfall variability: effect of grazing strategy on cattle production in a dry tropical savanna. Anim. Prod. Sci. 49, 85–99. https://doi.org/10.1071/EA07187.

O'Reagain, P.J., Bushell, J., Pahl, L., Scanlan, J.C., 2018. Wambiana Grazing Trial Phase 3: Stocking Strategies for Improving Carrying Capacity, Land Condition and Biodiversity Outcomes. B.ERM.0107. Meat and Livestock Australia. www.mla.com.au/research-and-development/reports/2018/part-2--wambiana-grazing-trial-phase-3-stocking-strategies-for-improving-carrying-capacity-land-condition-and-biodiversity-outcomes, North Sydney, Australia. URL.

Panda, S.S., Terrill, T.H., Mahapatra, A.K., Kelly, B., Morgan, E.R., van Wyck, J.A., 2020. Site-specific forage management of Serica Lespedeza: Geospatial technology-based forage quality and yield enhancement model development. Agriculture 10, 419. https://doi.org/10.3390/agriculture10090419.

Patterson, H.D., Thompson, R., 1971. Recovery of inter-block information when block sizes are unequal. Biometrika 58 (3), 545–554. https://doi.org/10.1093/biomet/58.3.545.

Paxton, G., 2019. Towards Greater Drought Preparedness in Queensland Grazing: Lessons from Qualitative Interviews and Discourse Analysis. Department of Environment and Science, Brisbane, Queensland. URL: data.longpaddock.qld.gov.au/static/dcap/DCAP2+DES3+Social+science+report+FINAL.pdf (accessed 23 November 2021).

Pettorelli, N., Ryan, S., Mueller, T., Bunnefeld, N., Jędrzejewska, B., Lima, M., Kausrud, K., 2011. The normalized difference vegetation index (NDVI): unforeseen success in animal ecology. Clim. Res. 46, 15–27. https://doi.org/10.3354/cr00936.

Phillips, R., Beeri, O., Scholljegerdes, E., Bjergaard, D., Hendrickson, J., 2009. Integration of geospatial and cattle nutrition information to estimate paddock grazing capacity in Northern US prairie. Agric. Syst. 100 (1-3), 72–79. https://doi.org/10.1016/j.agsy.2009.01.002.

Poppi, D.P., Minson, D.J., Ternouth, J.H., 1981. Studies of cattle and sheep eating leaf and fractions of grasses. I The voluntary intake, digestibility and retention time in the reticulo-rumen. Aust. J. Agric. Res. 32, 99–108. https://doi.org/10.1071/AR9810099.

Pringle, M.J., 2013. Robust prediction of time-integrated NDVI. Int. J. Remote Sens. 34 (13), 4791–4811. https://doi.org/10.1080/01431161.2013.782117.

R Core Team, 2020. R: A Language and Environment for Statistical Computing. R Foundation for Statistical Computing. r-project.org, Vienna, Austria. URL (accessed 23 November 2021).

Ryan, S.J., Cross, P.C., Winnie, J., Hay, C., Bowers, J., Getz, W.M., 2012. The utility of normalized difference vegetation index for predicting african buffalo forage quality. J. Wildlife Manage. 76 (7), 1499–1508. https://doi.org/10.1002/jwmg.407.

Scarth, P., Röder, A, Schmidt, M., 2010. Tracking grazing pressure and climate interaction—the role of Landsat fractional cover in time series analysis. In: Proceedings of Australasian Remote Sensing and Photogrammetry Conference, Alice Springs, 13–17 September. URL: figshare.com/articles/Tracking_Grazing_Pressure_and_Climate_Interaction_-_The_Role_of_Landsat_Fractional_Cover_in_Time_Series_Analysis/94250/1 (accessed 23 November 2021).

Schmidt, M., Carter, J., Stone, G., O'Reagain, P., 2016. Integration of optical and X-band radar data for pasture biomass estimation in an open savannah woodland. Remote Sens. 8, 989. https://doi.org/10.3390/rs8120989.

Siebert, B.D., Kennedy, P.M., 1972. The utilization of spear grass (*Heteropogon contortus*). I. Factors limiting intake and utilization by cattle and sheep. Aust. J. Agr. Res. 23, 35–44. https://doi.org/10.1071/AR9720045.

Standing Committee on Agriculture, Ruminants Subcommittee, 1990. Feeding Standards for Australian Livestock: Ruminants. CSIRO Publications, Melbourne.

Tolleson, D.R., Angerer, J.P., Kreuter, U.P., Sawyer, J.E., 2020. Growing degree day: noninvasive remotely sensed method to monitor diet crude protein in free-ranging cattle. Rangeland Ecol. Manage. 73 (2), 234–242. https://doi.org/10.1016/j.rama.2019.12.001.

Tucker, C.J., 1979. Red and photographic infrared linear combinations for monitoring vegetation. Remote Sens. Environ. 8 (2), 127–150. https://doi.org/10.1016/0034-4257(79)90013-0.

Villamuelas, M., Fernández, N., Albanell, E., Gálvez-Cerón, A., Bartholomé, J., Mentaberre, G., López-Olvera, J.R., Fernández-Aguilar, X., Colom-Cadena, A., López-Martín, J.M., Pérez-Barbería, J., Garel, M., Marco, I., Serrano, E., 2016. The Enhanced Vegetation Index (EVI) as a proxy for diet quality and composition in a mountain ungulate. Ecol. Indic. 61, 658–666. https://doi.org/10.1016/j.ecolind.2015.10.017.

Webster, R., Oliver, M.A., 2001. Geostatistics for Environmental Scientists. John Wiley & Sons Ltd, Chichester.

Wood, S.N., 2017. Generalized Additive Models: An Introduction with R, 2nd ed. Chapman and Hall/CRC, Philadelphia.

Zengeya, F.M., Mutanga, O., Murwira, A., 2013. Linking remotely sensed forage quality estimates from WorldView-2 multispectral data with cattle distribution in a savanna landscape. Int. J. Appl. Earth Obs. 21, 513–524. https://doi.org/10.1016/j.jag.2012.07.008.

Zhu, Z., Wang, S., Woodcock, C.E., 2015. Improvement and expansion of the Fmask algorithm: cloud, cloud shadow, and snow detection for Landsats 4–7, 8, and Sentinel 2 images. Remote Sens. Environ. 159, 269–277. https://doi.org/10.1016/j.rse.2014.12.014.